SUPPLEMENTARY FIGURE LEGENDS

Supplementary Figure 1: **Alexa Fluor 555-PCNA rescues primer extension in PCNA depleted *Xenopus laevis* egg extracts.** (A) An aliquot of LSS (low speed supernatant of *Xenopus laevis* egg extracts) or purified recombinant His6-xPCNA (0.024 ug) protein were loaded on 8% SDS-PAGE and analyzed by western blot using either antibodies against xPCNA (day 38, rabbit B) or pre-immune as a control (rabbit B). (B) Anti-PCNA western analysis of PCNA remaining in egg cytosolic extracts after 4 subsequent rounds of depletion with mock or anti-xPCNA polyclonal antibody shown in (A). After 4 rounds with specific antibody, the endogenous xPCNA is depleted to below 0.25% of starting concentration. (C) 15 ng/μL of M13 mp18 ssDNA (NEB) was primer extended by mock or PCNA-depleted extracts in the presence of [α^{32}P] dATP with or without supplementation of 333 nM mock or Alexa Fluor 555-PCNA trimer. The reaction was stopped at 15, 30, 60 and 120 minutes and the DNA was subjected to TBE-agarose gel electrophoresis. After drying, gels were subjected to autoradiography. The two bands represent supercoiled and nicked circular double-stranded M13 DNA. (D) The normalized replication efficiency was calculated by comparing the integrated counts per lane to the 120 minute time point of mock depleted sample.

Supplementary Figure 2: **Sample of typical motions of a DNA bound QDot versus sample of motions typically observed for PCNA-QDot complex.** (A) Kymograph of site-specific anti-digoxigenin QDot bound to doubly tethered λ DNA (stained with Sytox Orange in last image in panel). Position of QDot tracked in (B) is indicated with arrow. Frame rate is 19 Hz. (B) Relative positions of the tracked QDot along the *x* axis (normal to DNA long axis) and *y* axis (parallel to DNA long axis). (C) Relative position of the tracked particle along the *y* axis *versus* time. (D) Mean-square displacement *versus* time and fitting of points $n = 2$ to 10 reveals that the particle is not diffusing. (E) Kymograph of a diffusing PCNA-QDot complex on doubly tethered λ DNA (stained with Sytox Orange in last image in panel). Frame rate is 4 Hz. (B) Observed positions of the tracked particle along the *x* axis (normal to DNA long axis) and *y* axis (parallel to DNA long axis). (C) Observed position of the tracked particle along the *y* axis versus time. (D) Mean square displacement versus time and fitting of points $n = 2$ to 10 reveals that the particle is diffusing with a diffusion coefficient of 0.84 $\mu m^2/s$.

Supplementary Figure 3: **Observed and simulated step *n* to step *n* + 1 correlation and step size distributions justify assumption of at least 100 substeps per step in the 50 ms time interval used in simulations.** Notice that the observed step size distribution for the PCNA-QDot complex shown in (A) best resembles simulations with greater than 500 substeps per 250 ms interval shown in (D and E). (A) Right side of panel: Step sizes observed for PCNA-QDot complex sliding in 150 mM potassium glutamate buffer ($n = 4669$) with 250 ms time interval reveal a normal distribution. Left side of panel: Scatter plot of size of step *n* to size of step $n + 1$ shows no correlation between subsequent step sizes. (B) Right side of panel: Step sizes simulated for a two-speed stepper with $f_{hel} = 0.98$ based on predicted maximum diffusion coefficients for non-helical and helical sliding in buffer of viscosity $\eta = 1$ and assuming 5 substeps per 250 ms interval (or 1 substep per 50 ms) ($n = 9800$) predict predominantly small steps with a tail of very large steps. Left side of panel: The simulation predicts that large steps are most likely to be followed by very small steps, characteristics not seen in the observed PCNA-QDot step size distribution. (C) Right side of panel: Step sizes similarly simulated assuming 50 substeps per 250 ms interval (or 5 substeps per 50 ms) ($n = 9800$) predict a population of very small steps not seen in the observed PCNA-QDot distributions. Left side of panel: The size of step *n* is now not correlated with the size of step $n + 1$. (D) Right side of panel: Step size distribution similarly simulated assuming 500 substeps per 250 ms interval (100 substeps per 50 ms) ($n = 9800$) finally begins to resemble the observed step size data for PCNA-QDot complexes. Left side of panel:

The size of step n is now not correlated with the size of step $n + 1$. (E) Right side of panel: Step sizes similarly simulated assuming 5000 substeps per 250 ms interval (1000 substeps per 50 ms) (n = 9800) also resemble the observed step size data for PCNA-QDot complexes. Left side of panel: The size of step n is now not correlated with the size of step $n + 1$.

Supplementary Figure 4: **Assembling and characterizing the surface-to-bead double tethers.** (A) Cartoon depicting a surface-to-bead double tether. The biotinylated end of the Biotin-Lambda-Digoxigenin functionalized DNA molecule is bound to the streptavidin-covered surface of the PEG-passivated coverslip. The other end is bound by an anti-digoxigenin Fab fragment functionalized bead. Finally, the bead is bound to the surface via a bi-functional DNA oligomer (Bio-Dig Oligo) that was introduced in the presence of flow to stretch the DNA bead tether. (B) Scatter plot of DNA tether to tether lengths from a typical experiment shows that on average the surface-to-bead double tethers (n = 25) are better stretched (Mean Extension ± SEM = 12.6 ± 0.5 μm or 76.8 ± 2.8 % of contour length) than double surface tethers (n = 101) (Mean Extension ± SEM = 11.2 ± 0.1 μm or 68.1 ± 0.7% of contour length). If DNA molecules stretched to less than 10 um are excluded (they are likely not used for diffusion coefficient determination because imaging movement on slack DNAs is too difficult), the mean extension of the surface-to-bead double tethers is 13.3 ± 0.2 μm or 81.2 ± 1.5% of contour length and for double surface tethers is 11.5 ± 0.1 μm or 70.3 ± 0.5% of contour length. (C) A scale model (DNA thickness not to scale) of the surface-to-bead double tether reveals that a PCNA-QDot complex should be well away from the surface at the high end of the surface-to-bead double tether. (D) A Z-stack of images of Sytox Orange stained DNA, starting below the coverslip surface to the top of the bead, reveals that the DNA is rising away from the surface as shown in (B). Note that a singly tethered DNA is a random coil in the absence of flow.

Supplementary Figure 5: **Control for surface interactions: PCNA-QDot complex sliding on surface-to-bead double tethers.** (A) Kymograph of PCNA-QDot complex diffusing on a surface-to-bead tether. Imaging at 4 Hz. The focus was held steady on surface bound QDots. Notice that when the PCNA-QDot complex travels near the bead its diffraction limited image broadens due to defocusing as it travels away from the surface. (B) Observed positions of the tracked PCNA-QDot complex along the y axis (parallel to DNA long axis). The magenta line corresponds to the part of the trajectory shown in the kymograph in (A). (C) Mean square displacement versus time of the particle shown in (A) and (B) and fitting of points t = 0.5 to 2.5 reveals that the particle is diffusing with an apparent diffusion coefficient of 0.506 $\mu m^2/s$. (D) Scatter plot of apparent diffusion coefficients of PCNA-QDot complexes from 8 surface-to-bead tethers (Mean ± SEM = 0.83 ± 0.13 $\mu m^2/s$, n = 8) or of QDot-Alexa-PCNA or PCNA-QDot complexes on double surface tethers (Mean ± SEM = 0.55 ± 0.04 $\mu m^2/s$ and 0.43 ± 0.04 $\mu m^2/s$ respectively) reveals that raising the DNA off of the surface has no effect on the diffusion coefficient of PCNA after correcting for the higher extension of the surface-to-bead double tether (see text) . (E) Top panel: Mean step size for PCNA-QDot complexes diffusing on surface-to-bead tethers as a function of distance away from the center of the bead reveals that step size is relatively constant across the length of the DNA. This suggests that surface interactions have a negligible effect on PCNA-QDot sliding. Bottom panel: Number of steps originating from the specified position along the DNA away from the bead (total of 1747 steps analyzed). Note that the bead's size and brightness inhibit tracking of particles in its immediate vicinity (0 to 2 μm away from the center.)

SUPPLEMENTARY METHODS

Site specific labeling of biotin-lambda-biotin- To site-specifically label the biotin-lambda-biotin DNA with quantum dots, we used a protocol based on the work of Kuhn and Frank-Kamenetskii (1). Treatment of biotin-lambda-biotin DNA with the sequence-specific Nt.Bst.NBI nicking endonuclease results in nicked DNA with some of these nicks occurring on the same strand and closely spaced. The oligonucleotides between closely spaced nicks can be replaced with modified oligonucleotides of the same sequence via a strand-displacement reaction and subsequent ligation. Nicking reactions with Nt.Bst.NBI (NEB, 20 units) were performed on biotin-lambda-biotin DNA (2.5 μg) at 55 °C for 2 hours in buffer 3 (NEB). The nicked DNA was mixed with 100-fold excess of a 13-base oligonucleotide (IDT) modified with a 5' digoxigenin (5'-digoxigenin-TTCAGAGTCTGAC-3'), heated at 50 °C for 10 minutes and then slowly cooled to room temperature, resulting in the highly efficient replacement of the native sequence. Ligation was performed for 2 hours at room temperature using T4 ligase. This DNA was flow stretched using the same conditions as described above. The digoxigenin was detected by flowing in and then washing out a solution of 1 nM quantum dots (QDot; Invitrogen) which were functionalized with anti-digoxigenin Fab fragment (Roche) using the Invitrogen QDot Antibody Conjugation Kit.

Assembly and Characterization of Surface-to-Bead Double Tethers- We assembled surface-to-bead double tethers, where one end of the DNA is raised approximately 0.5 μm off of the coverslip surface, to ascertain whether the proximity of the surface affects the apparent diffusion coefficient. First, we prepared biotin-lambda-digoxigenin as described in the main text except that either the BL1 or BL2 oligomer was replaced with DL1- 5'-AGGTCGCCGCCC-Digoxigenin-3' or DL2- 5'GGGCGGCGACT-Digoxigenin-3' (IDT). To assemble the bead tethers (see cartoon in Supplementary Figure 4A), we first flowed a 3 pM solution of the functionalized DNA in Buffer A with 150 mM potassium glutamate past the coverslip surface. Next, a 2 nM solution of anti-digoxigenin Fab fragment functionalized 1-μm beads (2) also in Buffer A with 150 mM potassium glutamate was drawn in. After the free beads are washed away, most of the remaining biotin-lamda-digoxigenin DNA was bound to both the surface and a 1-μm bead. Finally, in order to keep the DNA stretched in the absence of flow, we 'stapled' the beads to the surface by flowing in a custom bifunctional oligo (5'-Biotin-CCCCCCCCCC-Digoxigenin-3' (IDT)) at 400 nM at 25 uL/min. The oligomer couples the anti-digoxigenin beads to the biotinylated surface. Thus we prepared well stretched DNAs whose mean end-to-bead distance in the absence of flow was 12.6 μm ± 0.5 μm (corresponding to 76.8 ± 2.8 % of contour length of lambda B-form DNA) (or for DNA likely used for tracking, the mean end to end distance was 13.3 ± 0.2 μm corresponding to 81.2 ± 1.5 % of contour length) (Supplementary Figure 4B). In this orientation, the DNA is well above the coverslip surface at the bead proximal end as illustrate to scale (DNA thickness not to scale) with a PCNA-QDot complex in Supplementary Figure 4C. Supplementary Figure 4D shows a Sytox stained surface-to-bead tether. Each image corresponds to a different focal plane, demonstrating that the bead-proximal end of the DNA is elevated from the surface.

SUPPLEMENTARY TEXT

Surface interactions do not slow PCNA-QDot complex sliding

We studied PCNA sliding on surface-to-bead tethers to ascertain whether proximity to the surface artificially decreases the apparent diffusion coefficient. Alexa Fluor 555-PCNA was loaded on the surface-to-bead double tethers as before and was subsequently labeled with QDots. After washing and stopping the flow, QDots were used for imaging PCNA sliding due to their higher brightness and longer photobleaching lifetime. The surface-to-bead double tethers rise in Z axis (the axis of focus) (Supplementary Figure 4D). Thus, the diffusing complex moves up and down

quickly in the Z-axis as it travels along the DNA (Y-axis). Since this motion is unpredictable and rapid, we chose to maintain focus on the surface (using surface bound QDots as fiducial markers) while imaging PCNA-QDot sliding (Supplementary Figure 5A). We determined the position of the complex at each time point by 2D Gaussian fitting to find the centroid of point spread function. For 8 sliding events that we observed and tracked successfully, and using the same fitting criteria as before, we determined the mean diffusion coefficient to be 0.83 ± 0.13 $\mu m^2/s$ ($\pm$ SEM) (Supplementary Figure 5 B,C,D). Although this is 1.5-fold higher than Alexa-PCNA-QDot sliding on double surface tethers, the extra extension of the surface-to-bead double tethers as compared to the surface tethers fully accounts for the discrepancy. Knowing that the mean extension of double surface tethers is 70.3% and surface-to-bead double tethers is 81.2%, the diffusion coefficient in basepairs of Alexa-PCNA-Qdot complexes are $1.06 \pm 0.10 \times 10^7$ bp^2/s and $1.20 \pm .19 \times 10^7$ bp^2/s respectively. Furthermore, when we calculate the mean step size as a function of distance away from the bead (1747 steps analyzed), we see no significant difference in the size of the steps originating from positions close to the bead versus close to the surface tethered end (Supplementary Figure 5E). Taken together, these data confirm that the apparent diffusion coefficients observed for PCNA and PCNA-QDot sliding on double surface tethers are not significantly affected by their proximity to the surface.

SUPPLEMENTARY REFERENCES

1. Kuhn, H., and Frank-Kamenetskii, M. D. (2008) *Nucleic Acids Res* **36**(7), e40
2. Lee, J.-B., Hite, R. K., Hamdan, S. M., Sunney Xie, X., Richardson, C. C., and van Oijen, A. M. (2006) *Nature* **439**(7076), 621-624

Supplementary Figure 1

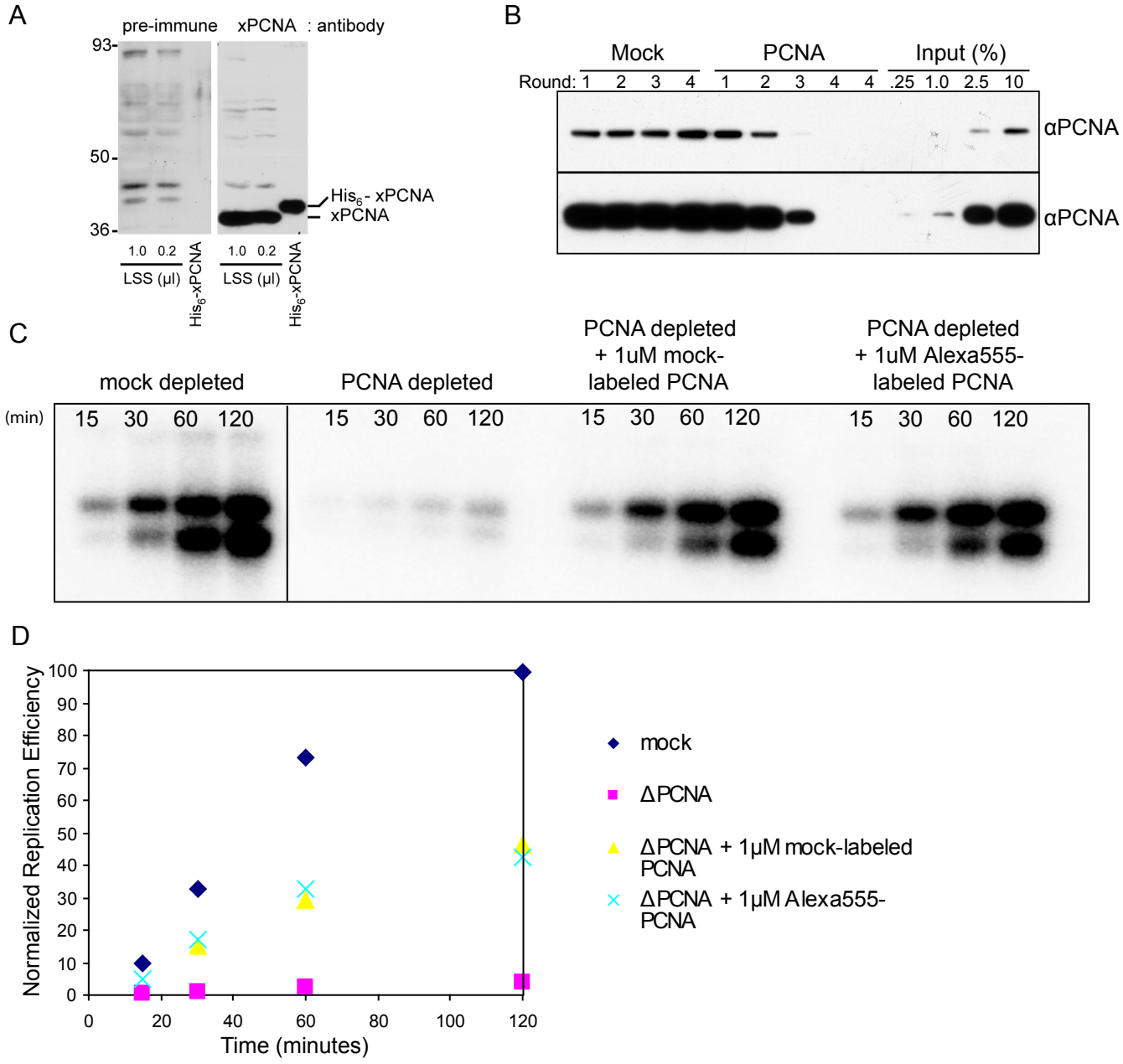

Supplementary Figure 2

A DNA immobilized QDot (frame rate 19 Hz)

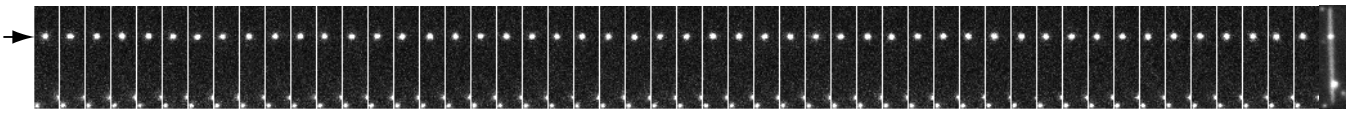

B

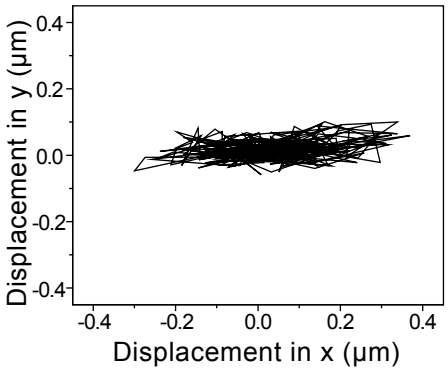

C

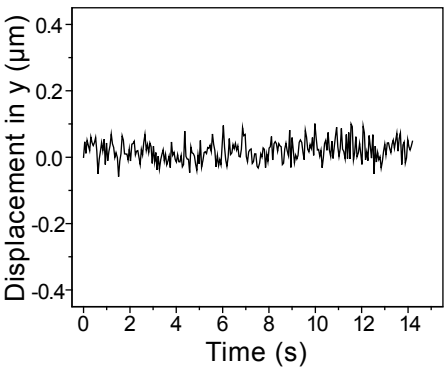

D

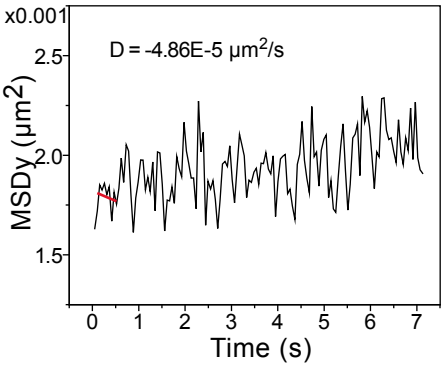

E PCNA-QDot motions (4 Hz)

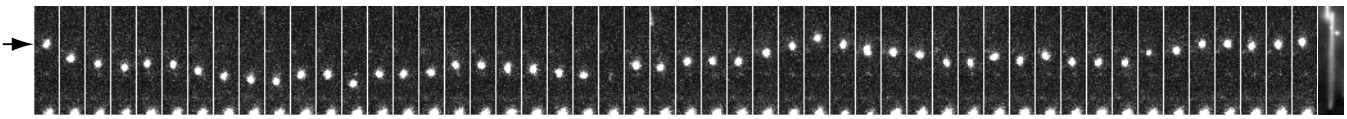

F

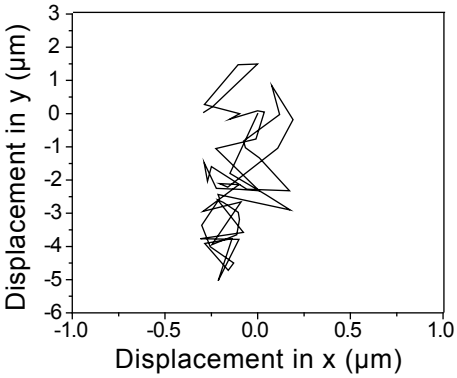

G

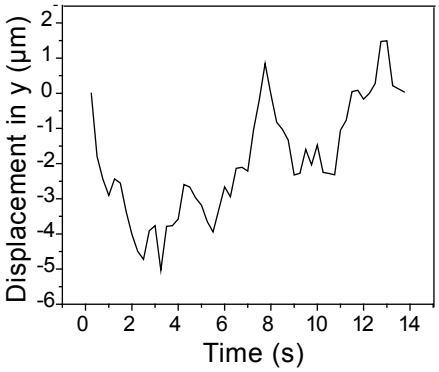

H

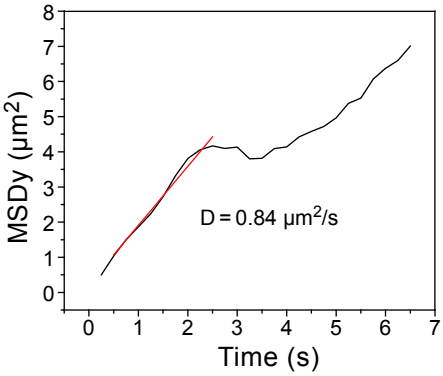

Supplementary Figure 3

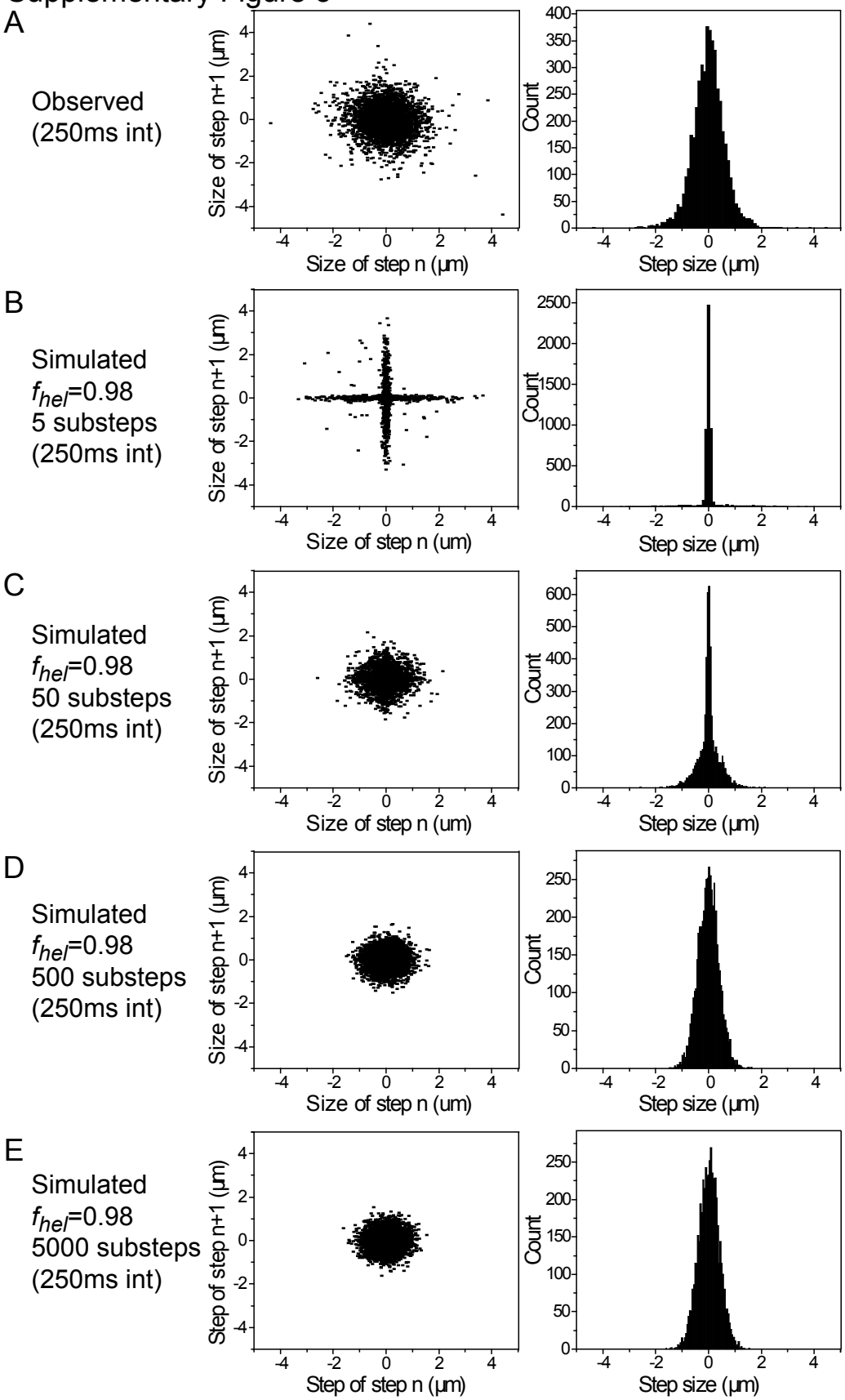

Supplementary Figure 4

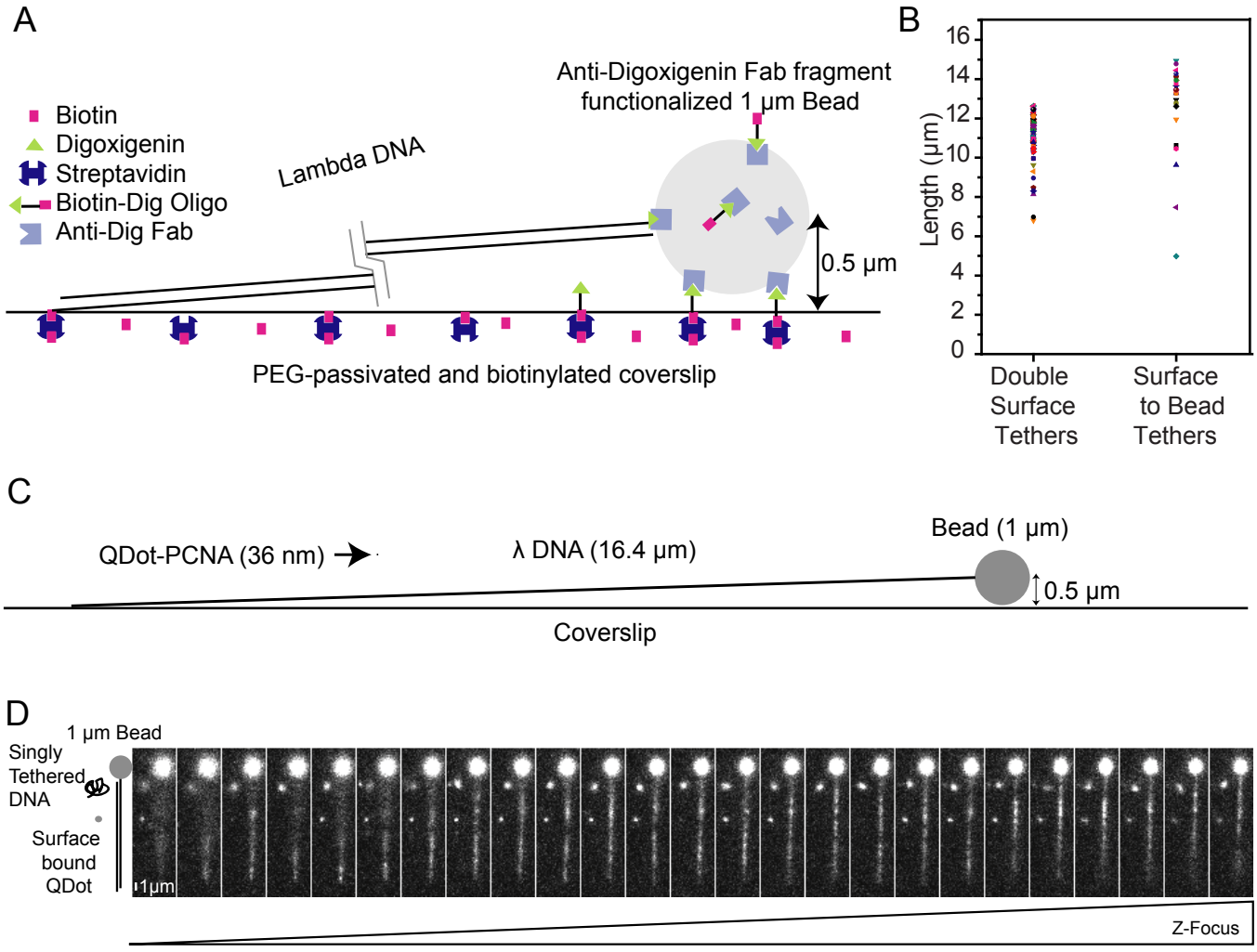
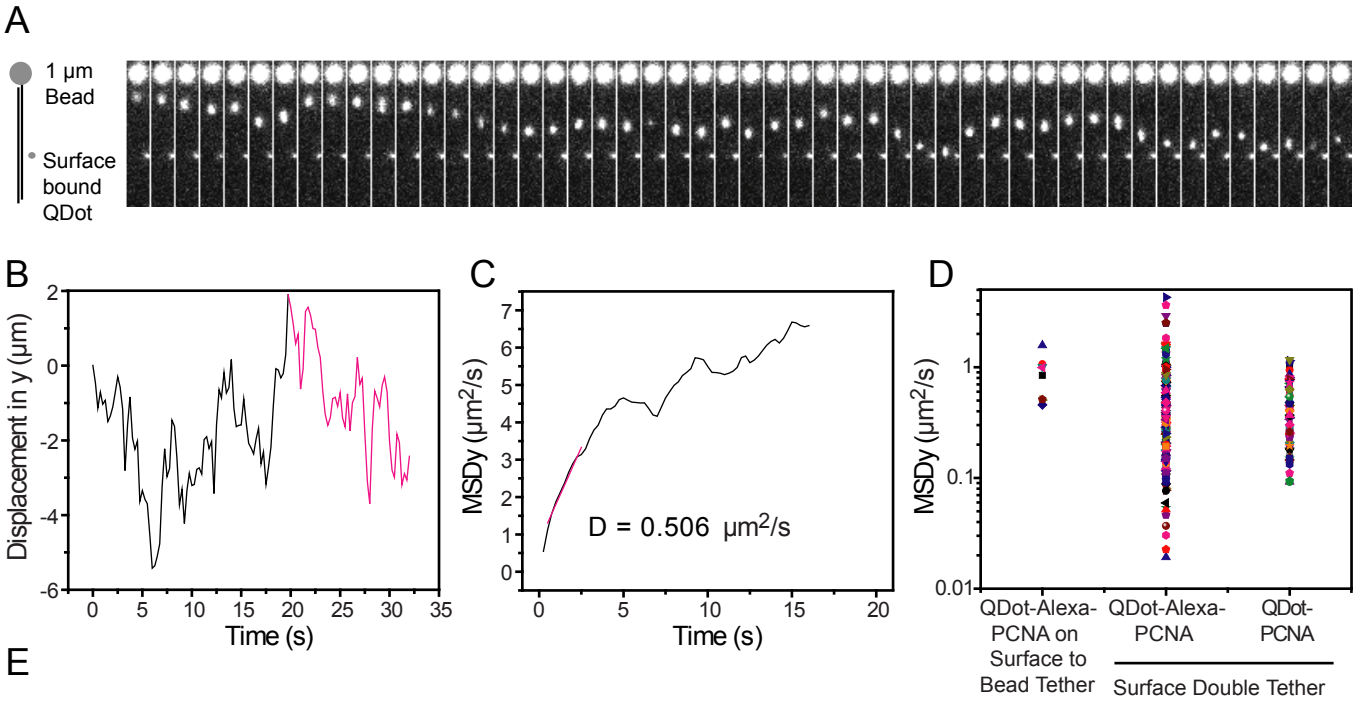
Supplementary Figure 5